

---

# Data Upcycling Knowledge Distillation for Image Super-Resolution

---

Yun Zhang<sup>1,2</sup>, Wei Li<sup>1</sup>, Simiao Li<sup>1</sup>, Jie Hu<sup>1</sup>, Hanting Chen<sup>1</sup>,  
Hailing Wang<sup>1</sup>, Zhijun Tu<sup>1</sup>, Wenjia Wang<sup>2</sup>, Bingyi Jing<sup>3</sup>, and Yunhe Wang<sup>1,†</sup>

<sup>1</sup>Huawei Noah’s Ark Lab

<sup>2</sup>DSA Thrust, INFO Hub, Hong Kong University of Science and Technology (GZ)

<sup>3</sup>Department of Statistics and Data Science, Southern University of Science and Technology

## Abstract

Knowledge distillation (KD) emerges as a challenging yet promising technique for compressing deep learning models, characterized by the transmission of extensive learning representations from proficient and computationally intensive teacher models to compact student models. However, only a handful of studies have endeavored to compress the models for single image super-resolution (SISR) through KD, with their effects on student model enhancement remaining marginal. In this paper, we put forth an approach from the perspective of efficient data utilization, namely, the Data Upcycling Knowledge Distillation (DUKD) which facilitates the student model by the prior knowledge teacher provided via upcycled in-domain data derived from their inputs. This upcycling process is realized through two efficient image zooming operations and invertible data augmentations which introduce the label consistency regularization to the field of KD for SISR and substantially boosts student model’s generalization. The DUKD, due to its versatility, can be applied across a broad spectrum of teacher-student architectures. Comprehensive experiments across diverse benchmarks demonstrate that our proposed DUKD method significantly outperforms previous art, exemplified by an increase of up to 0.5dB in PSNR over baselines methods, and a 67% parameters reduced RCAN model’s performance remaining on par with that of the RCAN teacher model.

## 1 Introduction

Single image super-resolution (SISR) is a fundamental but challenging task within the field of computer vision (CV), aiming to reconstruct high-resolution (HR) images from their low-resolution (LR) counterparts [30, 58, 29, 19, 39]. Over the past decade, convolutional neural networks (CNNs) [7, 25, 30, 58] and Transformers [29, 51, 48, 55] have demonstrated remarkable success in SISR tasks. Despite the impressive performance of deep learning-based SISR models, their practical deployment is typically hindered by the requirement of high computational resources and memory consumption [61]. Consequently, there has been a growing interest in the development of SISR model compression methods to facilitate real-world applications, particularly on resource-limited devices.

Knowledge Distillation (KD) is a powerful model compression technique that can substantially reduce the computation costs and memory requirements and improve the performance of the student model by transferring knowledge from the well-performed but cumbersome teacher model to the light and compact student model [8, 22, 60]. Compared with other compression techniques such as the quantization [12, 21, 23, 5, 50], pruning [1, 45, 33] and the neural architectures search (NAS) [49,

---

<sup>†</sup>Corresponding author.

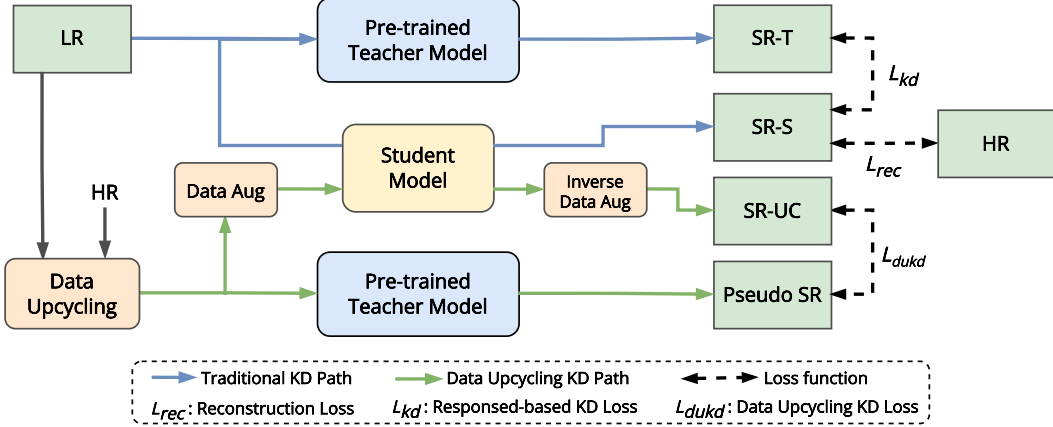


Figure 1: Framework of the DUKD method. DUKD facilitates the student by the prior knowledge provided by the teacher through upcycled in-domain data. The proposed invertible data augmentation paradigm makes the label consistency regularization applicable in the field of KD for SR and further enhance the generalization capability of the student. Details of data upcycling and invertible data augmentations are demonstrated in Fig.3.

17, 11], the KD has recently emerged as one of the most flourishing approach and can be incorporated with the these methods to further improve the student models.

The efficacy of KD has been well-established in natural language processing (NLP) [13, 10, 41, 24] and high-level CV tasks [37, 44, 3, 57, 20, 32]. However, its application in SISR tasks is comparatively less explored [15, 47, 8, 60, 28]. And the utilization of response-based KD methods [16] or those steadily effective on high-level CV tasks [40, 53, 54] display marginal improvements or may even yield detrimental effects when used for compressing SISR models, as noted by He et al. [15].

Prior KD methods specifically tailored for SISR have primarily utilized feature-based distillation, directly distilling the network intermediate feature maps [15] or through a pre-trained feature extracting network like VGG [52], and aiming to transfer a larger volume of knowledge from teacher to student. However, the effectiveness of these approaches remains somewhat constrained. Furthermore, feature-based distillation demands a certain level of architectural similarity between the teacher and student models and is incompatible with Transformer-based SR models. These methods often struggle to effectively convey the teacher model’s “dark knowledge”, resulting in a student model that does not fully encapsulate the teacher’s capabilities.

In this work, we take a distinctively innovative approach to KD for SISR, shifting the paradigm from various knowledge type to a more efficient data utilization. We present the *Data Upcycling Knowledge Distillation (DUKD)*, a simple yet highly effective KD framework for SISR. At the heart of this novel framework is the concept of *data upcycling*, which allows the teacher model to transfer its knowledge to the student model through the use of upcycled data. This process expands the boundaries of knowledge transfer, permitting the student model to harness the teacher model’s capabilities beyond the mere alignment of intermediate layers or original training data. Moreover, we introduce the concept of label consistency regularization to the field of KD for SISR, by employing *invertible data augmentations*. It further augments the student model’s generalization capabilities, enforcing consistency with the teacher model’s predictions, regardless of augmentations to the input data. The student, therefore, is exposed to a diverse range of inputs, enhancing its ability to learn and generalize. The implemented data augmentations include horizontal and vertical flip, 90° rotations, and color inversion, which are readily invertible and allow for consistency with the teacher model’s outputs. The universality of the proposed DUKD framework significantly broadens its applicability, enabling its use across various teacher-student architectures.

In summary, our main contributions are three-fold:

- We propose DUKD, a general KD approach that is capable of compressing and accelerating various SR networks. By leveraging the “dark knowledge” of the teacher model, our

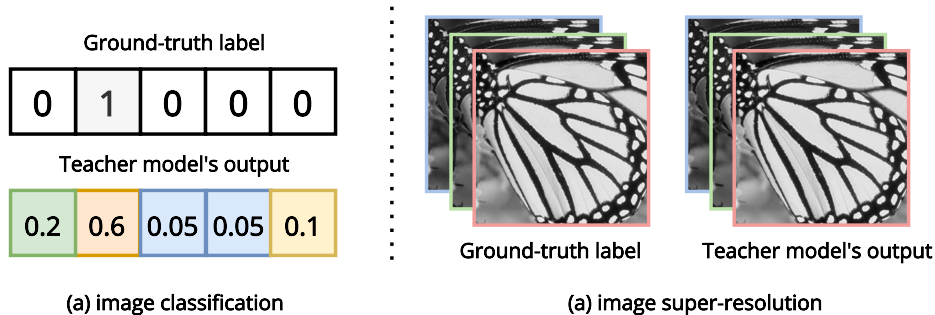


Figure 2: Comparison of the GT labels and teacher model’s output in the KD of image classification (#class = 5) and super-resolution tasks. The latter has higher dimension target labels and more similar supervision signals from GT label and teacher model’s response.

approach allows for the education of the student model via upcycled in-domain data, thereby enriching its learning process.

- We present invertible data augmentations, a novel application of label consistency regularization in the KD field. This ensures that the student model’s outputs align with those of the teacher model, regardless of input modifications. This expansion of input diversity ultimately enhances the student model’s generalization abilities.
- Our proposed DUKD, as shown through comprehensive experiments on various datasets and SR architectures, applies broadly to multiple teacher-student configurations, promising a cutting-edge KD approach for SISR. Remarkably, an RCAN student model, despite a reduction of 67% in parameters and FLOPS, remain on par with its teacher and 2× faster.

## 2 Related Works

### 2.1 Deep Image Super-Resolution Methods

Deep Neural Networks (DNNs) have been instrumental in advancing the field of Image Super-Resolution (SR), demonstrating significant improvements. The seminal work of Dong et al. [6] introduced Convolutional Neural Networks (CNNs) to image SR with a three-layered model. The Very Deep Super Resolution (VDSR) model [25] later built on this, employing residual learning for increasing network depth. The Enhanced Deep Super Resolution (EDSR) model [30] further improved the design by simplifying the residual block [14]. Subsequent advancements included the Residual Channel Attention Network (RCAN)[58], which incorporated a residual-in-residual structure and a channel attention mechanism, and the FRANet model[31] that emphasized critical spatial contents. Later works by Mei et al. [35] and Zhang et al. [59] explored the potential of residual non-local attention and correlational feature integration for image restoration. The advent of the Transformer model has seen its application to image restoration, with notable works such as Image Processing Transformer (IPT)[4], SwinIR[29], Restormer [55], and Uformer [48]. However, despite their remarkable performance in SISR, both CNNs and Transformers still struggle with issues of memory consumption and computational overhead.

### 2.2 Knowledge Distillation for Single Image Super-Resolution

Among various model compression approaches, KD [16] has gained prominence as an effective technique, facilitating the transfer of “dark knowledge” from a cumbersome, well-performed teacher model to a compact and computationally efficient student model. The KD for SISR are different from and harder than KD for high-level CV tasks owing to 1) the greater dimension of target labels in SR tasks which complicates model optimization and 2) the significant similarity between the ground-truth (GT) label and teacher model’s output which leads to the issue of *supervision ambiguity*, as demonstrated in Fig. 2. They hinder the application of many traditional KD methods on this particular task. The Feature Affinity-based Knowledge Distillation (FAKD) [15] facilitates the distillation of second-order statistical information from the teacher model’s feature maps to the

student model. Zhang et al. [60] introduced a data-free KD framework, designed for scenarios where the training data of the teacher model remains inaccessible to the student model. The Contrastive Self-Distillation (CSD) [47] method trains the student model via channel splitting self-distillation, yet it is only applicable when the teacher and student models share the same network architecture and depth. Yao et al. [52] proposed to balance the student models’ ability on both reconstruction fidelity and perceptual quality by leveraging supervision from diverse types of teacher models. Our proposed DUKD improve the student model from a new perspective, emphasizing more on the role of data in the KD process.

### 3 Methodology

#### 3.1 Notations and Preliminaries

Let  $\mathcal{T}(x; \theta^t)$  and  $\mathcal{S}(x; \theta^s)$  be a teacher and a student model with parameters  $\theta^t$  and  $\theta^s$ . Given an input LR image  $I_{LR}^{(i)}$ , output SR images of the two networks are denoted by  $I_{SR}^{\mathcal{T}(i)} = \mathcal{T}(I_{LR}^{(i)}; \theta^t)$  and  $I_{SR}^{\mathcal{S}(i)} = \mathcal{S}(I_{LR}^{(i)}; \theta^s)$ , and the corresponding HR image is  $I_{HR}^{(i)}$ . The L1-norm reconstruction loss of student model is computed as:

$$L_{rec} = \|I_{SR}^{\mathcal{S}(i)} - I_{HR}^{(i)}\|_1. \quad (1)$$

And the response-based KD loss is

$$L_{kd} = \|I_{SR}^{\mathcal{S}(i)} - I_{SR}^{\mathcal{T}(i)}\|_1, \quad (2)$$

which is directly derived from the output of teacher and student models.

#### 3.2 Data Upcycling

The overall framework is demonstrated in Fig.1. It showcases how the pre-trained teacher model is not solely engaged in conventional knowledge distillation but also harnesses its capabilities to supervise the student model on upcycled data, bypassing the need for ground-truth HR counterparts. This is a significant departure from feature-based KD methods which primarily focus on the transfer of intermediate feature maps. Our method, on the other hand, emphasizes on the efficient utilization of data, and the teacher model’s capacity to direct the learning process through this upcycled data.

The procedure of data upcycling is partly conducted through two types of image zooming operations as illustrated in Fig.3 (a). The zoom-in operation is facilitated by randomly cropping a patch from the original HR image that is of equal size to the LR image. Conversely, the zoom-out operation is achieved through downsampling the LR image. For a given LR image, the output of the zoom-out operation is unique, but the zoom-in operation for HR images could result in various outcomes. Beyond random cropping, regions can also be alternatively selected based on their perceived difficulty as reflected by the teacher model’s reconstruction loss. However, this approach would induce higher computational costs in the training phase.

Through the implementation of these zooming operations, we are able to upcycle both the HR and LR images by generating alternative labels of in-domain upcycled data from the teacher model. This procedure allows for a more comprehensive exploitation of the limited data at hand, consequently enhancing the effectiveness of the teacher’s knowledge transfer to the student model. The DUKD thereby provides a more refined and data-centric approach to KD, reflecting its benefits in terms of efficient data utilization and superior performance in the context of SISR tasks.

The overall loss of our KD framework is constructed by adding one extra DUKD loss term computed on upcycled data to the reconstruction loss Eq. 1 and response-based KD loss Eq. 2. For the input  $(I_{LR}^{(i)}, I_{HR}^{(i)})$  image pair, denote the upcycled data as  $I_{LR_{zo}}^{(i)}, I_{HR_{zi}}^{(i)}$ ,

$$L_{dukd} = \|I_{SR_{zo}}^{\mathcal{S}(i)} - I_{SR_{zo}}^{\mathcal{T}(i)}\|_1 + \|I_{SR_{zi}}^{\mathcal{S}(i)} - I_{SR_{zi}}^{\mathcal{T}(i)}\|_1, \quad (3)$$

where  $I_{SR_{zo}}^{\mathcal{S}(i)} = \mathcal{S}(I_{LR_{zo}}^{(i)}; \theta^s)$ ,  $I_{SR_{zo}}^{\mathcal{T}(i)} = \mathcal{T}(I_{LR_{zo}}^{(i)}; \theta^t)$  and the other terms are computed in a similar manner.



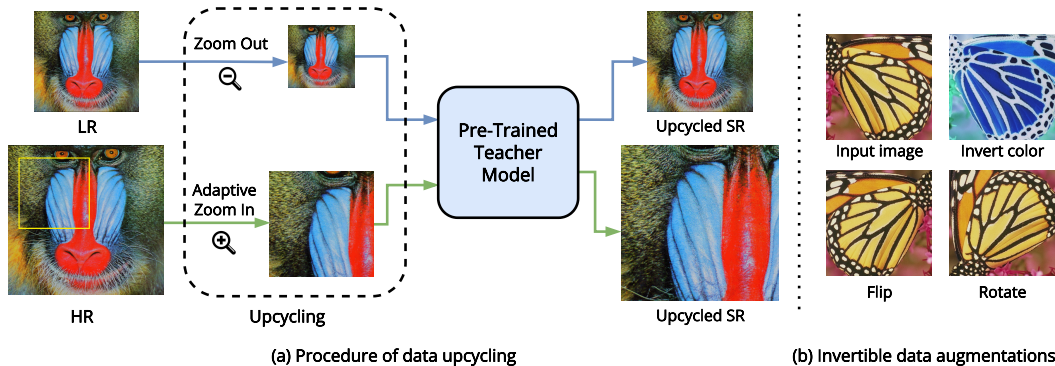


Figure 3: Demonstration of data upcycling and invertible data augmentations. The generated in-domain upcycled data allows the teacher to convey prior knowledge to the student. The invertible data augmentations impose label consistency regularization between teacher and student model and further improve its generalization capability.

### 3.3 Invertible Data Augmentations

Data augmentation reduces the generalization error by compelling a model to learn invariant representations under diverse transformations applied to the input image. In high-level CV tasks, various data augmentations are typically employed on model inputs, based on the assumption that data augmentation transformations should not affect model predictions given the same input [27, 42, 9, 36]. In knowledge distillation, if only the student model’s input is augmented while teacher’s is not, the student model is trained towards consistency with a more powerful teacher model generating outputs based on non-augmented inputs which inherently possess superior quality compared to those derived from augmented inputs. Therefore, when training student with the upcycled data, we perform data augmentations on the input of the student model only, and invert those augmentations on student’s output to make them compatible with the teacher model’s responses.

In order to preserve the reversibility of the augmentations, it is vital that crucial pixel-level information within the original image is maintained after augmentation. Denote the data augmentation operation as  $\mathcal{D}(\cdot)$ , the self-inverse condition  $\mathcal{D}(\mathcal{D}(I)) = I$  defines an invertible operation. Hence, a number of popular image augmentations, such as blurring, cutout, brightness adjustment, and cropping, are not applicable as they do not meet this prerequisite. Instead, we employ two geometric transformations, horizontal and vertical flips and  $90^\circ$  rotations, along with a novel color inversion transformation that subtracts pixel intensity values of the input image from 255 (or 1 if normalized). This color inversion transformation, being invertible, maintains the relative magnitude among pixel values, and also prompts the student models to be more sensitive to essential structural features such as lines and edges. Figure 3 (b) illustrates the three types of invertible data augmentations employed in DUKD. augmentations applied to the original input data; 2) the invertible data augmentation is a new approach to utilize data augmentations in KD which imposes the label consistency regularization for the first time.

Our proposed DUKD framework diverges significantly from conventional data augmentation or expansion techniques in the following ways: Firstly, the data upcycling procedure is intimately intertwined with KD, wherein the HR label corresponding to the upcycled in-domain LR image is generated by the teacher model. This distinct characteristic contrasts with traditional data augmentation techniques that typically operate on the original input data independent of any teacher model, and is different to the dataset expansion that introduces extra out-domain data. In DUKD, data upcycling is not merely an operation to increase the volume or diversity of the data, but rather serves a more significant purpose - it acts as a vehicle for the teacher model to transmit its knowledge to the student model. This unique procedure allows the student model to learn more effectively from the teacher model’s responses on the upcycled data, thus enhancing its performance. Secondly, DUKD also introduces the invertible data augmentation, a novel approach to the utilization of data augmentations in KD. Unlike conventional data augmentation operations, which aim to increase the robustness of models by presenting varied versions of input data, invertible data augmentation is specifically tailored for KD. It imposes the label consistency regularization for the first time, which enforces the student model to produce consistent outputs with the teacher model, even when the inputs are transformed through various invertible augmentations. It only allows the student model to

Table 1: SR model specifications and statistics ( $\times 4$  scale). The FLOPs and frames per second (FPS) are computed with  $3 \times 256 \times 256$  input image and FPS is computed on a single V100 GPU with 64GB memory. The block denotes the number of residual blocks (in each residual group) for EDSR and RCAN models or residual swin transformer blocks for SwinIR models.

Model	Role	Network			FLOPs (G)	#Params	FPS
		Channel	Block	Group			
EDSR	Teacher	256	32	-	3293.35	43.09 M	3.233
	Student	64	32	-	207.28	2.70 M	33.958
RCAN	Teacher	64	20	10	1044.03	15.59 M	6.162
	Student	64	6	10	366.98	5.17 M	12.337
SwinIR	Teacher	180	6	-	861.27	11.90 M	0.459
	Student	60	4	-	121.48	1.24 M	0.874

learn the teacher’s invariant features across transformations but also encourages the student model to generalize better to unseen data.

## 4 Experiments

### 4.1 Experiment Settings

**Backbones and Baselines.** We use EDSR [30], RCAN [58] and SwinIR [29] as backbone models to verify the effectiveness of DUKD and compare it with some existing KD methods. The specifications of teacher and student networks and some statistics including FLOPs, number of parameters and model inference speed (FPS) are presented in Table 1. We compare our KD framework with five baseline training and KD methods: train from scratch, response-based KD [16], FAKD [15], and CSD [47]. To evaluate the performance of SISR models, we calculate the peak signal-to-noise ratio (PSNR) and the structural similarity index (SSIM) on the Y channel of the YCbCr color space.

**Training Details.** The SR models are trained with the 800 training images from DIV2K [43] and evaluated on four benchmark datasets: Set5 [2], Set14 [56], BSD100 [34], and Urban100 [18]. The LR images used for training were obtained by down-sampling the HR images with the bicubic degradation. During training, the input LR image is randomly cropped into  $48 \times 48$  patches and augmented with random horizontal and vertical flips and rotations. For FAKD and CSD methods, we follow the hyperparameters setting specified in their paper and train the models by ourselves if checkpoint is not provided, as particularly noted in the results section. The zoom in operation of DUKD is conducted by randomly cropping for simplicity. The zoom out is not used when training SwinIR models since the result image would be too small to be valid input for SwinIR. Models are trained with ADAM optimizer [26] with  $\beta_1 = 0.9$ ,  $\beta_2 = 0.99$  and  $\epsilon = 10^{-8}$ , with a batch size of 16 and a total of  $2.5 \times 10^5$  updates. The initial learning rate is set to  $10^{-4}$  and is decayed by a factor of 10 at every  $10^5$  iterations. We implemented the proposed kd method with the BasicSR [46] and PyTorch 1.10 framework [38] and trained them using 4 NVIDIA V100 GPUs.

### 4.2 Results and Comparison

**Comparison with Baseline Methods.** The quantitative result (PSNR and SSIM) is shown in table 2, comparing three SR backbone networks in  $\times 2$ ,  $\times 3$ , and  $\times 4$  scales. The following conclusions can be drawn from these results: (1) Existing KD techniques have limited effects, with some even leading to the deterioration of the student model. For instance, EDSR models trained with FAKD sometimes underperform models trained from scratch. (2) Our proposed KD framework consistently outperforms the existing KD baseline methods in all experimental settings. For example, when compared with the response-based KD method, the average PSNR gains of the three types of networks on the Urban100 test set for  $\times 2$ ,  $\times 3$ , and  $\times 4$  scales are 0.43 dB, 0.31 dB, 0.31 dB, respectively. In Fig. 4 we demonstrates the model’s PSNR improvements derived from our KD method under different settings of model compression rates and student model sizes. Benefits for the students distilled from a larger teacher is more significant, as our KD method can effectively transfer more capabilities from teachers. In Fig. 5 we demonstrates the effectiveness of different KD methods by comparing the similarity of

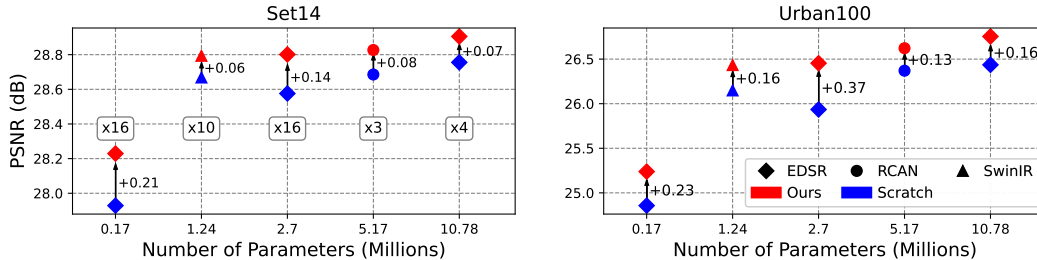


Figure 4: PSNR improvements v.s number of parameters of different SR models ( $\times 4$  scale) on Set14 and Urban100 test sets. Compression rates in terms of number of parameters are indicated in the left figure.

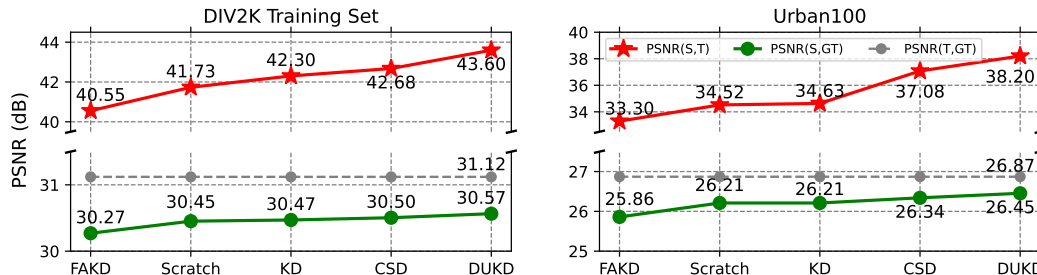


Figure 5: Evaluating the agreement between student and teacher models of various knowledge distillation on  $\times 4$  scale EDSR models. The student model trained with DUKD can effectively fit the teacher model on training set and perform like it on the unseen data.

student’s output towards teacher’s on the training and Urban100 testing sets to evaluate if the student learns well to mimic the teacher model. It shows that DUKD makes the student not only effectively fit the teacher model on training set but also imitate it on the test sets, so that the student model’s outputs gets closer to GT as well.

**Experiment Results on Heterogeneous Settings.** We extend the experiments to heterogeneous settings where the teacher and student models have different network architectures, as presented in table 3. Such cross-architecture distillation is not applicable for other feature-based KD or self-distillation methods, while DUKD can still effectively improve the student models. For instance, compared to the RCAN model trained from scratch, utilizing DUKD with an EDSR or SwinIR teacher model yields an increase in PSNR by 0.22dB at  $\times 4$  scale on Urban100 test set.

**Visual Comparison.** As shown in Fig.6, we compare our KD method with others on four images from Urban100 dataset in terms of output qualitative results of EDSR student model of  $\times 4$  scale. To underscore the differences in detailed pattern and texture reconstruction, we have compared relatively small cropped images, with PSNR calculated solely on these cropped parts. Metrics in the caption are calculated by considering only the cropped part. Generally, a higher PSNR aligns with superior subjective image quality. For the reconstruction of textures (e.g. lines, edges and complex patterns), the model trained with DUKD yields outputs that are both sharper and more similar to the HR images, owing to the data upcycling procedure which boosts the model’s generalizability .

### 4.3 Ablation Analysis

**Effect of data upcycling and invertible data augmentations.** The data upcycling and invertible data augmentations enhance the student model by a large margin. The influence of each component is ablated in Tab 4. We use EDSR model with 64 channels and 32 residual blocks as the teacher, and one with a quarter of channels numbers as the student. The result shows that adopting data upcycling and invertible data augmentations could lead to significant performance improvement upon prior KD methods, whether used individually or together. For example, simply upcycling data by zoom-in draws 0.31dB PSNR increment on Urban100 test set, and adding zoom-out and invertible data augmentations yields an additional 0.16dB improvement. This compelling result underscores

Table 2: Quantitative results in different experiment settings. The KD refers to response-based knowledge distillation in this table. The best results are **highlighted**. Asterisk \* denotes the model is retrained by ourselves as checkpoint is not available.

Scale	Model	Method	Set5		Set14		BSD100		Urban100	
			PSNR	SSIM	PSNR	SSIM	PSNR	SSIM	PSNR	SSIM
×2	EDSR	Scratch	38.00	0.9605	33.57	0.9171	32.17	0.8996	31.96	0.9268
		KD	38.04	0.9606	33.58	0.9172	32.19	0.8998	31.98	0.9269
		FAKD*	37.97	0.9604	33.47	0.9170	32.11	0.8987	31.66	0.9240
		CSD*	38.06	0.9607	33.65	0.9179	32.22	0.9004	32.26	0.9300
		DUKD	<b>38.15</b>	<b>0.9610</b>	<b>33.80</b>	<b>0.9195</b>	<b>32.27</b>	<b>0.9007</b>	<b>32.53</b>	<b>0.9320</b>
	RCAN	Scratch	38.13	0.9610	33.78	0.9194	32.26	0.9007	32.63	0.9327
		KD	38.18	0.9611	33.83	0.9197	32.29	0.9010	32.67	0.9329
		FAKD	38.16	0.9611	33.82	0.9190	32.27	0.9010	32.53	0.9320
		DUKD	<b>38.23</b>	<b>0.9614</b>	<b>33.90</b>	<b>0.9201</b>	<b>32.33</b>	<b>0.9016</b>	<b>32.87</b>	<b>0.9349</b>
	SwinIR	Scratch	38.01	0.9607	33.57	0.9178	32.19	0.9000	32.05	0.9279
		KD	38.04	0.9608	33.61	0.9184	32.22	0.9003	32.09	0.9282
		DUKD	<b>38.13</b>	<b>0.9610</b>	<b>33.78</b>	<b>0.9194</b>	<b>32.26</b>	<b>0.9007</b>	<b>32.63</b>	<b>0.9327</b>
×3	EDSR	Scratch	34.39	0.9270	30.32	0.8417	29.08	0.8046	27.99	0.8489
		KD	34.43	0.9273	30.34	0.8422	29.10	0.8050	28.00	0.8491
		FAKD*	34.20	0.9259	30.24	0.8409	29.02	0.8031	27.69	0.8434
		CSD*	34.45	0.9275	30.32	0.8430	29.11	0.8061	28.21	0.8549
		DUKD	<b>34.59</b>	<b>0.9287</b>	<b>30.47</b>	<b>0.8448</b>	<b>29.20</b>	<b>0.8073</b>	<b>28.44</b>	<b>0.8578</b>
	RCAN	Scratch	34.61	0.9288	30.45	0.8444	29.18	0.8074	28.59	0.8610
		KD	34.61	0.9291	30.47	0.8447	29.21	0.8080	28.62	0.8612
		FAKD	34.65	0.9291	30.45	0.8442	29.21	0.8087	28.52	0.8602
		DUKD	<b>34.74</b>	<b>0.9296</b>	<b>30.54</b>	<b>0.8458</b>	<b>29.25</b>	<b>0.8088</b>	<b>28.79</b>	<b>0.8646</b>
	SwinIR	Scratch	34.41	0.9273	30.43	0.8437	29.12	0.8062	28.20	0.8537
		KD	34.44	0.9275	30.45	0.8443	29.14	0.8066	28.23	0.8545
		DUKD	<b>34.55</b>	<b>0.9285</b>	<b>30.53</b>	<b>0.8456</b>	<b>29.20</b>	<b>0.8080</b>	<b>28.53</b>	<b>0.8604</b>
×4	EDSR	Scratch	32.29	0.8965	28.68	0.7840	27.64	0.7380	26.21	0.7893
		KD	32.30	0.8965	28.70	0.7842	27.64	0.7382	26.21	0.7897
		FAKD*	32.07	0.8938	28.57	0.7819	27.55	0.7358	25.86	0.7798
		CSD	32.34	0.8974	28.72	0.7856	27.68	0.7396	26.34	0.7948
		DUKD	<b>32.47</b>	<b>0.8981</b>	<b>28.80</b>	<b>0.7866</b>	<b>27.71</b>	<b>0.7403</b>	<b>26.45</b>	<b>0.7963</b>
	RCAN	Scratch	32.31	0.8970	28.69	0.7840	27.64	0.7380	26.37	0.7950
		KD	32.45	0.8980	28.76	0.7860	27.67	0.7400	26.49	0.7980
		FAKD	32.46	0.8980	28.75	0.7860	27.68	0.7400	26.42	0.7970
		DUKD	<b>32.56</b>	<b>0.8990</b>	<b>28.83</b>	<b>0.7870</b>	<b>27.72</b>	<b>0.7410</b>	<b>26.62</b>	<b>0.8020</b>
	SwinIR	Scratch	32.31	0.8955	28.67	0.7833	27.61	0.7379	26.15	0.7884
		KD	32.27	0.8954	28.67	0.7833	27.62	0.7380	26.15	0.7887
		DUKD	<b>32.41</b>	<b>0.8973</b>	<b>28.79</b>	<b>0.7860</b>	<b>27.69</b>	<b>0.7405</b>	<b>26.43</b>	<b>0.7972</b>

Table 3: The results of heterogeneous distillation using DUKD on the RCAN model at ×4 scale.

Teacher	Student	Set5		Set14		BSD100		Urban100	
		PSNR	SSIM	PSNR	SSIM	PSNR	SSIM	PSNR	SSIM
-	RCAN	32.31	0.8966	28.69	0.7842	27.64	0.7384	26.37	0.7949
EDSR	RCAN	32.51	0.8986	28.80	0.7868	27.71	0.7406	26.59	0.8014
SwinIR	RCAN	32.50	0.8986	28.82	0.7872	27.72	0.7408	26.59	0.8007

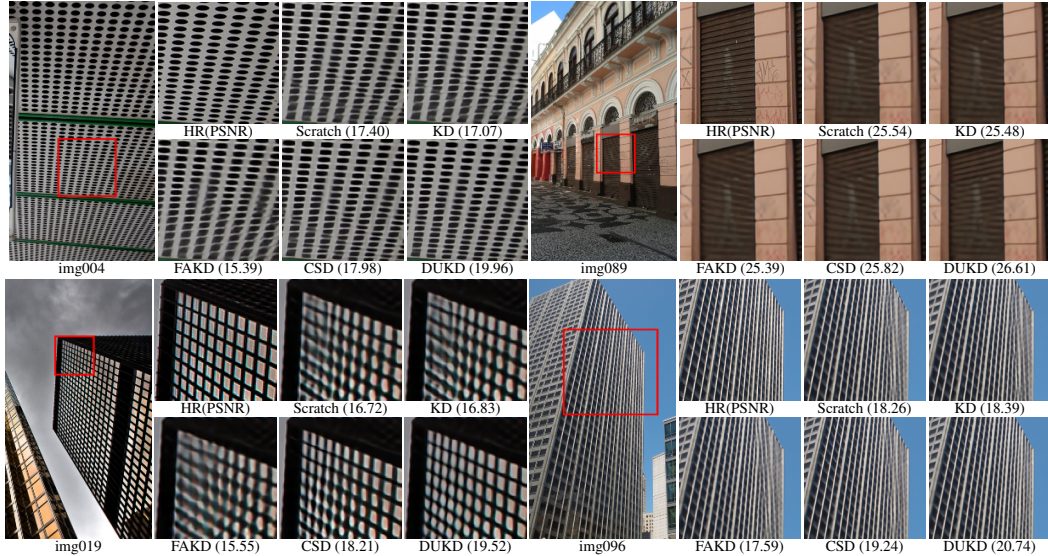


Figure 6: The  $\times 4$  super resolution results of EDSR models on img004, img019, img089 and img096 from Urban100. PSNRs of the cropped regions are annotated below each image.

Table 4: Ablation study of data upcycling mechanisms and reversible data augmentation.

Method	Set5		Set14		BSD100		Urban100		DIV2K Validation	
	PSNR	SSIM	PSNR	SSIM	PSNR	SSIM	PSNR	SSIM	PSNR	SSIM
Scratch	31.12	0.8782	27.93	0.7663	27.13	0.7217	24.86	0.7421	29.75	0.8215
Logits-KD	31.16	0.8791	27.95	0.7670	27.13	0.7223	24.87	0.7431	29.77	0.8223
FAKD	30.86	0.8735	27.79	0.7636	27.06	0.7190	24.75	0.7381	29.66	0.8196
Zoom In	31.51	0.8849	28.19	0.7726	27.29	0.7268	25.18	0.7551	29.98	0.8269
Zoom Out	31.54	0.8855	28.20	0.7725	27.29	0.7269	25.18	0.7552	29.97	0.8268
Zoom In + Zoom Out	31.55	0.8857	28.21	0.7727	27.30	0.7269	25.20	0.7558	29.99	0.8269
Zoom In+DA	31.59	0.8863	28.23	0.7730	27.31	0.7274	25.24	0.7571	30.00	0.8273
Zoom In + Zoom Out + DA	31.73	0.8883	28.29	0.7745	27.36	0.7288	25.34	0.7609	30.06	0.8286

the potential of our DUKD approach in maximizing the effectiveness of knowledge transfer in the KD framework, offering a promising avenue for future exploration in the domain of efficient model compression and acceleration.

## 5 Limitation and Discussion

While our DUKD methodology exhibits superior performance on an array of benchmark datasets for SISR task, its applicability to other CV tasks is inherently constrained due to the distinct input-output relationships that characterize different learning tasks. Specifically, super-resolution models possess a unique property that their output can be recursively used as input, a characteristic that is not universally met in other tasks. This renders the data upcycling procedure, as introduced in our study, somewhat ineffective when extended to tasks such as objection detection, image classification, deblurring, deraining, etc. Moreover, while our approach focuses on enhancing data utilization, it does not explore the potential benefits from feature distillation. Though our experiment results suggest that DUKD outperforms traditional feature-based KD methods in SISR task, it does not imply that feature distillation is entirely dispensable. Indeed, an insightful exploration of the synergistic effects of data upcycling and feature distillation methods might lead to a further improvement of the student models.

## 6 Conclusion

In this work, we present DUKD, a simple yet significant KD framework for SISR that is universally applicable to a wide array of teacher-student architectures. Central to our approach is the novel

procedure of data upcycling, which we implement through the application of zoom-in and zoom-out operations to LR and HR images respectively. This data-centric method enables the teacher model to impart its latent knowledge effectively via this upcycled data. Beyond the data upcycling, we have also pioneered the introduction of label consistency regularization to the field of KD for SISR. This mechanism serves to further bolster the student model’s generalization capabilities, fortifying its learning process with an emphasis of stability and consistency. We have conducted extensive experiments across a variety of benchmark datasets and diverse SISR backbones. The consistent outperformance of DUKD in these tests endorses its promise as a robust and effective KD method for SISR tasks. In conclusion, our DUKD framework signifies an important paradigm shift from feature-based KD methods towards more efficient data utilization strategies, harnessing the power of data upcycling and label consistency regularization to push the boundaries of SISR model performance.

## References

- [1] S. Anwar, K. Hwang, and W. Sung. Structured pruning of deep convolutional neural networks. *ACM Journal on Emerging Technologies in Computing Systems (JETC)*, 13(3):1–18, 2017.
- [2] M. Bevilacqua, A. Roumy, C. Guillemot, and M. L. Alberi-Morel. Low-complexity single-image super-resolution based on nonnegative neighbor embedding. *BMVC*, 2012.
- [3] G. Chen, W. Choi, X. Yu, T. Han, and M. Chandraker. Learning efficient object detection models with knowledge distillation. *NeurIPS*, 30, 2017.
- [4] H. Chen, Y. Wang, T. Guo, C. Xu, Y. Deng, Z. Liu, S. Ma, C. Xu, C. Xu, and W. Gao. Pre-trained image processing transformer. In *CVPR*, pages 12299–12310, 2021.
- [5] M. Courbariaux, Y. Bengio, and J.-P. David. Binaryconnect: Training deep neural networks with binary weights during propagations. *NeurIPS*, 28, 2015.
- [6] C. Dong, C. C. Loy, K. He, and X. Tang. Learning a deep convolutional network for image super-resolution. In *ECCV*, pages 184–199. Springer, 2014.
- [7] C. Dong, C. C. Loy, K. He, and X. Tang. Image super-resolution using deep convolutional networks. *IEEE transactions on pattern analysis and machine intelligence*, 38(2):295–307, 2015.
- [8] Q. Gao, Y. Zhao, G. Li, and T. Tong. Image super-resolution using knowledge distillation. In *ACCV*, pages 527–541. Springer, 2019.
- [9] I. J. Goodfellow, J. Shlens, and C. Szegedy. Explaining and harnessing adversarial examples. *arXiv preprint arXiv:1412.6572*, 2014.
- [10] J. Gou, B. Yu, S. J. Maybank, and D. Tao. Knowledge distillation: A survey. *International Journal of Computer Vision*, 129:1789–1819, 2021.
- [11] Z. Guo, X. Zhang, H. Mu, W. Heng, Z. Liu, Y. Wei, and J. Sun. Single path one-shot neural architecture search with uniform sampling. In *ECCV*, pages 544–560. Springer, 2020.
- [12] S. Gupta, A. Agrawal, K. Gopalakrishnan, and P. Narayanan. Deep learning with limited numerical precision. In *ICML*, pages 1737–1746. PMLR, 2015.
- [13] S. Hahn and H. Choi. Self-knowledge distillation in natural language processing. *arXiv preprint arXiv:1908.01851*, 2019.
- [14] K. He, X. Zhang, S. Ren, and J. Sun. Deep residual learning for image recognition. In *CVPR*, pages 770–778, 2016.
- [15] Z. He, T. Dai, J. Lu, Y. Jiang, and S.-T. Xia. Fakd: Feature-affinity based knowledge distillation for efficient image super-resolution. In *ICIP*, pages 518–522. IEEE, 2020.
- [16] G. Hinton, O. Vinyals, and J. Dean. Distilling the knowledge in a neural network. *arXiv preprint arXiv:1503.02531*, 2015.



- [17] A. Howard, M. Sandler, G. Chu, L.-C. Chen, B. Chen, M. Tan, W. Wang, Y. Zhu, R. Pang, V. Vasudevan, et al. Searching for mobilenetv3. In *ICCV*, pages 1314–1324, 2019.
- [18] J.-B. Huang, A. Singh, and N. Ahuja. Single image super-resolution from transformed self-exemplars. In *CVPR*, pages 5197–5206, 2015.
- [19] X. Huang, W. Li, J. Hu, H. Chen, and Y. Wang. Refsr-nerf: Towards high fidelity and super resolution view synthesis. In *Proceedings of the IEEE/CVF Conference on Computer Vision and Pattern Recognition (CVPR)*, pages 8244–8253, June 2023.
- [20] Z. Huang and N. Wang. Like what you like: Knowledge distill via neuron selectivity transfer. *arXiv preprint arXiv:1707.01219*, 2017.
- [21] I. Hubara, M. Courbariaux, D. Soudry, R. El-Yaniv, and Y. Bengio. Binarized neural networks. *NeurIPS*, 29, 2016.
- [22] Z. Hui, X. Gao, Y. Yang, and X. Wang. Lightweight image super-resolution with information multi-distillation network. In *Proceedings of the 27th acm international conference on multimedia*, pages 2024–2032, 2019.
- [23] A. Ignatov, R. Timofte, M. Denna, and A. Younes. Real-time quantized image super-resolution on mobile npus, mobile ai 2021 challenge: Report. In *CVPR*, pages 2525–2534, 2021.
- [24] X. Jiao, Y. Yin, L. Shang, X. Jiang, X. Chen, L. Li, F. Wang, and Q. Liu. Tinybert: Distilling bert for natural language understanding. *arXiv preprint arXiv:1909.10351*, 2019.
- [25] J. Kim, J. K. Lee, and K. M. Lee. Accurate image super-resolution using very deep convolutional networks. In *Proceedings of the IEEE conference on computer vision and pattern recognition*, pages 1646–1654, 2016.
- [26] D. P. Kingma and J. Ba. Adam: A method for stochastic optimization. *arXiv preprint arXiv:1412.6980*, 2014.
- [27] S. Laine and T. Aila. Temporal ensembling for semi-supervised learning. *arXiv preprint arXiv:1610.02242*, 2016.
- [28] W. Lee, J. Lee, D. Kim, and B. Ham. Learning with privileged information for efficient image super-resolution. In *ECCV*, pages 465–482. Springer, 2020.
- [29] J. Liang, J. Cao, G. Sun, K. Zhang, L. Van Gool, and R. Timofte. Swinir: Image restoration using swin transformer. In *ICCV*, pages 1833–1844, 2021.
- [30] B. Lim, S. Son, H. Kim, S. Nah, and K. Mu Lee. Enhanced deep residual networks for single image super-resolution. In *CVPR*, pages 136–144, 2017.
- [31] J. Liu, W. Zhang, Y. Tang, J. Tang, and G. Wu. Residual feature aggregation network for image super-resolution. In *CVPR*, pages 2359–2368, 2020.
- [32] Y. Liu, K. Chen, C. Liu, Z. Qin, Z. Luo, and J. Wang. Structured knowledge distillation for semantic segmentation. In *CVPR*, pages 2604–2613, 2019.
- [33] Z. Liu, H. Mu, X. Zhang, Z. Guo, X. Yang, K.-T. Cheng, and J. Sun. Metapruning: Meta learning for automatic neural network channel pruning. In *ICCV*, pages 3296–3305, 2019.
- [34] D. Martin, C. Fowlkes, D. Tal, and J. Malik. A database of human segmented natural images and its application to evaluating segmentation algorithms and measuring ecological statistics. In *ICCV*, volume 2, pages 416–423. IEEE, 2001.
- [35] Y. Mei, Y. Fan, Y. Zhou, L. Huang, T. S. Huang, and H. Shi. Image super-resolution with cross-scale non-local attention and exhaustive self-exemplars mining. In *CVPR*, pages 5690–5699, 2020.
- [36] T. Miyato, S.-i. Maeda, M. Koyama, and S. Ishii. Virtual adversarial training: a regularization method for supervised and semi-supervised learning. *IEEE transactions on pattern analysis and machine intelligence*, 41(8):1979–1993, 2018.

- [37] W. Park, D. Kim, Y. Lu, and M. Cho. Relational knowledge distillation. In *CVPR*, pages 3967–3976, 2019.
- [38] A. Paszke, S. Gross, F. Massa, A. Lerer, J. Bradbury, G. Chanan, T. Killeen, Z. Lin, N. Gimelshein, L. Antiga, et al. Pytorch: An imperative style, high-performance deep learning library. *NeurIPS*, 32, 2019.
- [39] J. Qiao, S. Lin, Y. Zhang, W. Li, H. Jie, G. He, C. Wang, and Z. Ma. Dcs-risr: Dynamic channel splitting for efficient real-world image super-resolution. *arXiv preprint arXiv:2212.07613*, 2022.
- [40] A. Romero, N. Ballas, S. E. Kahou, A. Chassang, C. Gatta, and Y. Bengio. Fitnets: Hints for thin deep nets. *arXiv preprint arXiv:1412.6550*, 2014.
- [41] V. Sanh, L. Debut, J. Chaumond, and T. Wolf. Distilbert, a distilled version of bert: smaller, faster, cheaper and lighter. *arXiv preprint arXiv:1910.01108*, 2019.
- [42] A. Tarvainen and H. Valpola. Mean teachers are better role models: Weight-averaged consistency targets improve semi-supervised deep learning results. *Advances in neural information processing systems*, 30, 2017.
- [43] R. Timofte, E. Agustsson, L. Van Gool, M.-H. Yang, and L. Zhang. Ntire 2017 challenge on single image super-resolution: Methods and results. In *CVPRW*, pages 114–125, 2017.
- [44] F. Tung and G. Mori. Similarity-preserving knowledge distillation. In *ICCV*, pages 1365–1374, 2019.
- [45] L. Wang, X. Dong, Y. Wang, X. Ying, Z. Lin, W. An, and Y. Guo. Exploring sparsity in image super-resolution for efficient inference. In *CVPR*, pages 4917–4926, 2021.
- [46] X. Wang, L. Xie, K. Yu, K. C. Chan, C. C. Loy, and C. Dong. BasicSR: Open source image and video restoration toolbox. <https://github.com/XPixelGroup/BasicSR>, 2022.
- [47] Y. Wang, S. Lin, Y. Qu, H. Wu, Z. Zhang, Y. Xie, and A. Yao. Towards compact single image super-resolution via contrastive self-distillation. *arXiv preprint arXiv:2105.11683*, 2021.
- [48] Z. Wang, X. Cun, J. Bao, W. Zhou, J. Liu, and H. Li. Uformer: A general u-shaped transformer for image restoration. In *CVPR*, pages 17683–17693, 2022.
- [49] B. Wu, X. Dai, P. Zhang, Y. Wang, F. Sun, Y. Wu, Y. Tian, P. Vajda, Y. Jia, and K. Keutzer. Fbnet: Hardware-aware efficient convnet design via differentiable neural architecture search. In *CVPR*, pages 10734–10742, 2019.
- [50] J. Wu, C. Leng, Y. Wang, Q. Hu, and J. Cheng. Quantized convolutional neural networks for mobile devices. In *CVPR*, pages 4820–4828, 2016.
- [51] F. Yang, H. Yang, J. Fu, H. Lu, and B. Guo. Learning texture transformer network for image super-resolution. In *CVPR*, pages 5791–5800, 2020.
- [52] G. Yao, Z. Li, B. Bhanu, Z. Kang, Z. Zhong, and Q. Zhang. Mtkdsr: Multi-teacher knowledge distillation for super resolution image reconstruction. *2022 26th ICPR*, pages 352–358, 2022.
- [53] J. Yim, D. Joo, J. Bae, and J. Kim. A gift from knowledge distillation: Fast optimization, network minimization and transfer learning. In *CVPR*, pages 4133–4141, 2017.
- [54] S. Zagoruyko and N. Komodakis. Paying more attention to attention: Improving the performance of convolutional neural networks via attention transfer. *arXiv preprint arXiv:1612.03928*, 2016.
- [55] S. W. Zamir, A. Arora, S. Khan, M. Hayat, F. S. Khan, and M.-H. Yang. Restormer: Efficient transformer for high-resolution image restoration. In *CVPR*, pages 5728–5739, 2022.
- [56] R. Zeyde, M. Elad, and M. Protter. On single image scale-up using sparse-representations. In *Curves and Surfaces: 7th International Conference, Avignon, France, June 24-30, 2010, Revised Selected Papers 7*, pages 711–730. Springer, 2012.



- [57] L. Zhang, J. Song, A. Gao, J. Chen, C. Bao, and K. Ma. Be your own teacher: Improve the performance of convolutional neural networks via self distillation. In *ICCV*, pages 3713–3722, 2019.
- [58] Y. Zhang, K. Li, K. Li, L. Wang, B. Zhong, and Y. Fu. Image super-resolution using very deep residual channel attention networks. In *ECCV*, pages 286–301, 2018.
- [59] Y. Zhang, K. Li, K. Li, B. Zhong, and Y. Fu. Residual non-local attention networks for image restoration. *arXiv preprint arXiv:1903.10082*, 2019.
- [60] Y. Zhang, H. Chen, X. Chen, Y. Deng, C. Xu, and Y. Wang. Data-free knowledge distillation for image super-resolution. In *CVPR*, pages 7852–7861, 2021.
- [61] Y. Zhang, H. Wang, C. Qin, and Y. Fu. Aligned structured sparsity learning for efficient image super-resolution. *NeurIPS*, 34:2695–2706, 2021.